Electronic Supplementary Material (ESI) for Nanoscale.
This journal is © The Royal Society of Chemistry 2022

Supporting Information

Precise regulation of defect concentration in MOF and its influence on photocatalytic overall water splitting

Changyan Guo [a], Tao Wang [a], Li Zhang [a, b*], Tingxiang Chen [a], Cheng Guo [a], Afaq Hassan [a], Naeem Akram [c], Yuli Kou [a], Jide Wang [a*]

[a] Key Laboratory of Oil and Gas Fine Chemicals, Ministry of Education & Xinjiang Uygur Autonomous Region, School of chemical engineering and technology, Xinjiang University, Urumqi, China

[b] Department of Chemical Engineering, Tiemenguan Vocational and Technical College, Korla, China

[c] School of Chemical Engineering, Minhaj University Lahore, Lahore (54000) Pakistan

*Corresponding author.

E-mail addresses: zhangltzy@sina.com (Li Zhang); awangjd@sina.cn (Jide Wang).

1. Materials and methods

1.1. Characterization of samples

The microtopography was observed via an FEI Magellan 400L XHR Field mission Scanning Electron Microscope (SEM). X-ray diffraction (XRD) patterns were obtained using a Rigaku D/max-ga X-ray diffractometer with Cu Kα radiation, which were recorded in the 2θ range of 5-80^{o} with a scan rate of 6^{o}/min. FT-IR spectra were recorded by a Bruker EQUINOX-55 FTIR instrument in a wavenumber range of 400-4000 cm^{-1} at room temperature. X-ray photoelectron spectroscopy (XPS) was conducted on a Thermo K-Alpha^{+} X-ray photoelectron spectrometer equipped with the monochromatic Al Kα (1486.8 eV) source. The electron paramagnetic resonance spectra (CW EPR) were recorded on the Bruker A300 instrument, which operates at X-band frequencies and is equipped with a cylindrical cavity, and operates at a 100 kHz field modulation. The surface area was calculated via N_2 adsorption-desorption isotherm measurements on an Autosorb iQ instrument, and pore size distribution was estimated through the analysis of the desorption portion of the isotherms using the DFT method. Thermogravimetric analysis (TGA) was carried out under an N_2 atmosphere at a heating rate of 10^{o}C/min up to 500^{o}C on the Shimadzu DTG-50 thermal analyzer. The UV-vis absorption spectra were acquired by using a UV-2550 spectrophotometer (Shimadzu). The Photoluminescence (PL) spectra were obtained on the FLS920 full-function steady-state/transient fluorescence spectrometer. UV-vis diffuse reflectance spectra (UV-vis DRS) recorded on a Unico UV-4802S and barium sulfate was used as the reference.

1.2. Photocatalytic reaction

The photocatalytic activity of samples was studied in the water oxidation system and water reduction system. The typical light-driven oxygen evolution reaction: catalyst (3-7 mg), $Na_2S_2O_8$ (10-40 mM) and NaOH (0.01-1 mM) solution were added to a reaction vessel. The typical light-driven hydrogen evolution reaction: catalyst (1-5 mg), EY dye (3-9 mg), TEOA (5%-15%) and distilled water were added to a reaction vessel. The reaction flask was sealed with a rubber septum and purged with argon gas for 10 min. The photocatalytic reaction was carried out by a 300 W Xe lamp equipped with a long-pass filter ($\lambda \geq 420$ nm). The produced gases were analyzed by a gas chromatography instrument (SHIMADZU GC-2014C) with a thermal conductivity detector (TCD, 5 Å molecular sieve column) and a column dimension (2 m × 4 mm) that Ar as the carrier gas.

1.3. Electrochemistry measurements

The electrochemical impedance spectroscopy (EIS) and transient photocurrent response were obtained in a standard three-electrode experimental system via a CHI760E electrochemical analyzer. The prepared fluorinated tin oxide glass (FTO) was used as the working electrodes, which conductive surface has 100 μL of 20 mg/mL catalyst and then obtained photoelectrodes were dried in the air for 12 hours. A saturated glycerol electrode (SCE) was used as the reference electrode and a platinum plate as the counter electrode.

2. FT-IR spectra

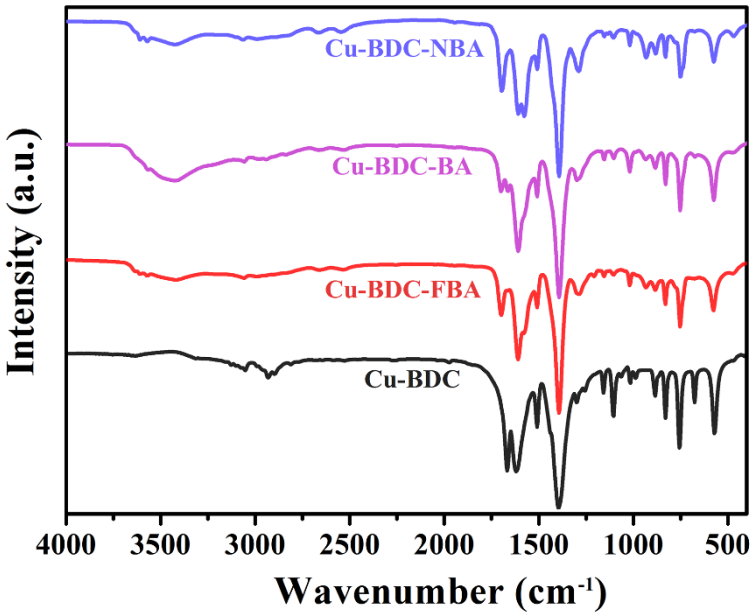

Fig. S1. FT-IR spectra of Cu-BDC and Cu-BDC variants.

3. TG analysis

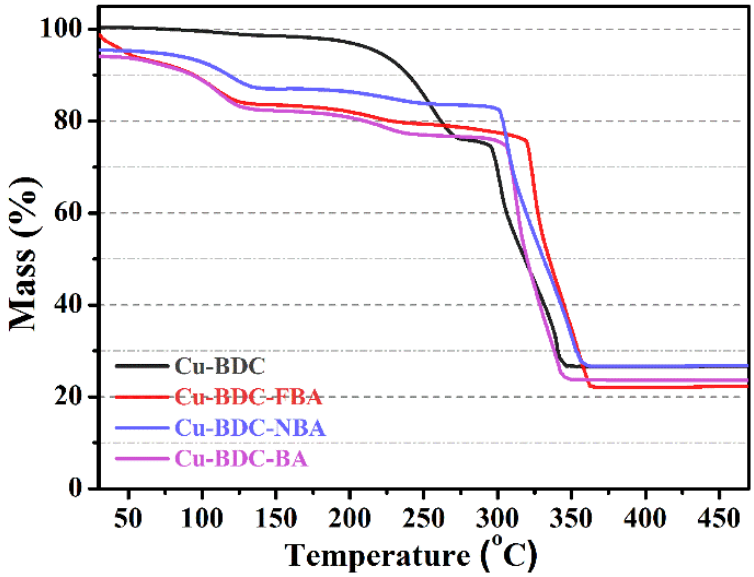

Fig. S2. TGA images of Cu-BDC and defective Cu-BDC samples.

4. XPS survey of samples

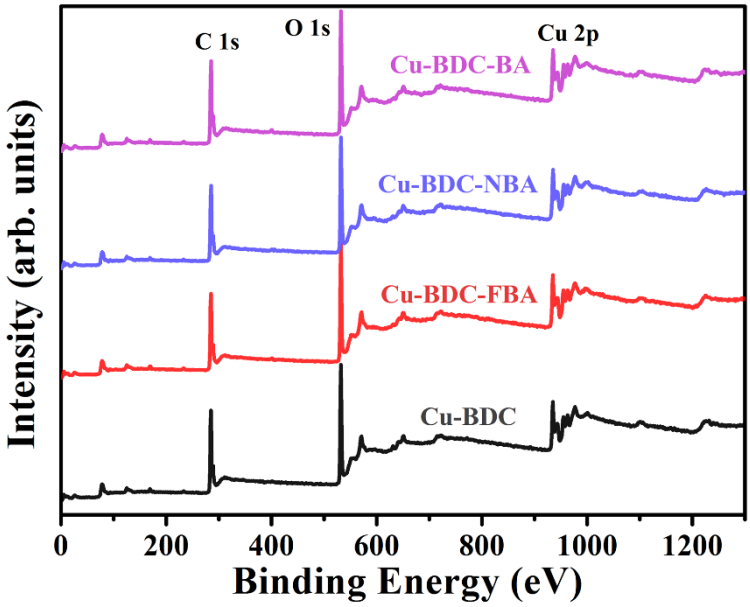

Fig. S3. XPS survey scans for Cu-BDC and Cu-BDC variants.

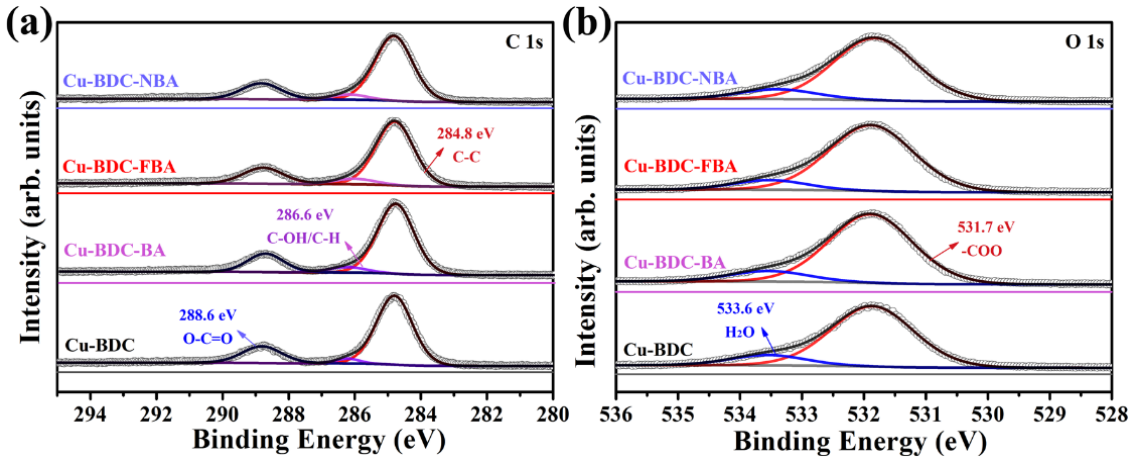

Fig. S4. (a) C 1s peaks of samples; (b) O 1s peaks of samples.

5. Control experimental

Table S1. Photocatalytic Oxygen Evolution over Cu-BDC-FBA under Different Conditions [a].

Variables	Trials	O_2 (μmol·g^{-1}·h^{-1})
Control experiment	no Cu-BDC-FBA	0
	no $Na_2S_2O_8$	0
	no NaOH	0
	no light	0
$Na_2S_2O_8$ amount [b]	10 mM	2598.3
	20 mM	**3112.5**
	30 mM	2885.1
NaOH amount [c]	0.01 mM	1896.8
	0.1 mM	**3115.6**
	1 mM	2598.3
Cu-BDC-FBA amount [d]	3	3015.5
	5	**3114.5**
	7	2952.2

[a] Performed with a volume of 10 mL NaOH solution, 20 mL of headspace, and a 300 W Xe lamp (λ ≥ 420 nm) illumination for 7 h.[b] Fixed reagents: 5 mg Cu-BDC-FBA and 0.1 mM NaOH solution. [c] Fixed reagents: 5 mg Cu-BDC-FBA and 20 mM $Na_2S_2O_8$. [d] Fixed reagents: 0.1 mM NaOH solution and 20 mM $Na_2S_2O_8$.

Table S2. Photocatalytic Hydrogen Production with Cu-BDC-FBA under Different Conditions [a].

Variables	Trials	H_2 (μmol·g^{-1}·h^{-1})
Control experiment	no Cu-BDC-FBA	0
	no TEOA	0
	no EY	0
	no light	0
TEOA amount [b]	2%	11850.4
	5%	**16830.5**
	10%	14256.0
EY amount [c]	**3 mg**	**2534.0**
	6 mg	16830.2
	9 mg	10250.2
Cu-BDC-FBA amount [d]	1	10352.1
	2	**16828.6**
	3	9821.5

[a] Performed with a volume of 10 mL (H_2O + TEOA), 20 mL of headspace, and a 300 W Xe lamp (λ ≥ 420 nm) illumination for 7 h.[b] Fixed reagents: 2 mg Cu-BDC-FBA and 6 mg EY. [c] Fixed reagents: 2 mg Cu-BDC-FBA and 5% TEOA. [d] Fixed reagents: 6 mg EY and 5% TEOA.

6. Band gap

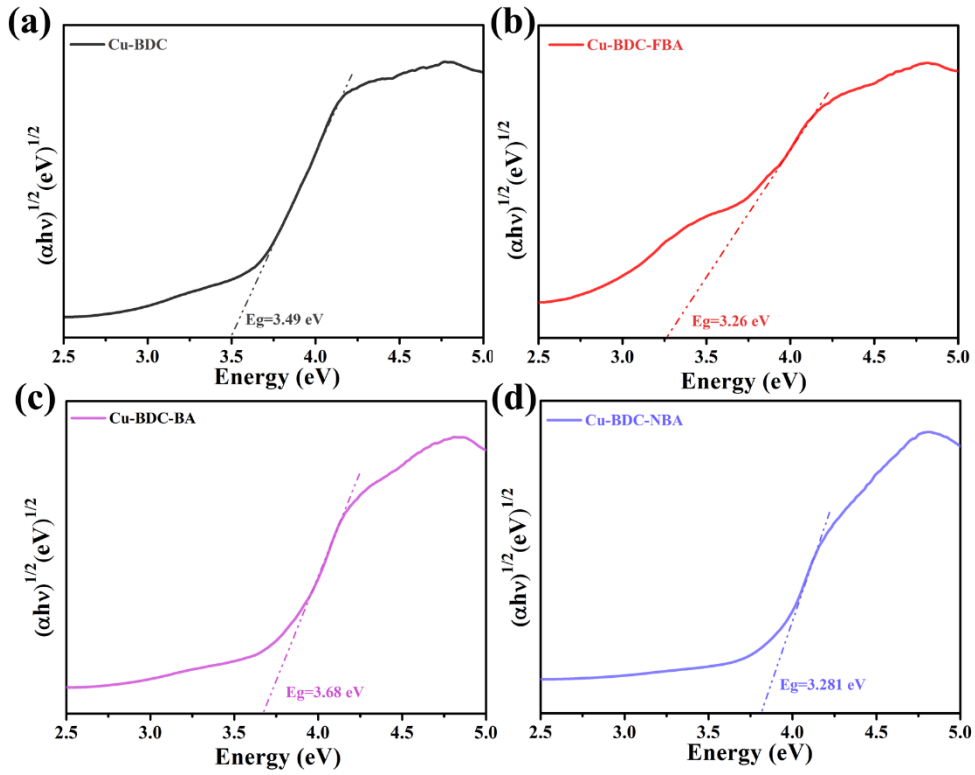

Fig. S5. Kubelka-Munk transformed diffuse reflectance spectra of samples: (a) Cu-BDC; (b) Cu-BDC-FBA; (c) Cu-BDC-BA; (d) Cu-BDC-NBA.

Table S3. Comparison of the catalytic performance of different catalysts.

Catalyst	Reaction condition	Evolved oxygen	Reaction condition	Evolved hydrogen	Ref.
Cu-BDC-FBA	5 mg catalyst; 20 mM $Na_2S_2O_8$; 10 mL 0.1 M NaOH aqueous solution (pH 13); total reaction volume 10 mL; 300 W Xe lamp ($\lambda \geq 420$ nm).	3114 $\mu mol \cdot g^{-1} \cdot h^{-1}$	2 mg catalyst; 6 mg EY; 5% TEOA aqueous solution; total reaction volume 10 mL; 300 W Xe lamp ($\lambda \geq 420$ nm).	16829 $\mu mol \cdot g^{-1} \cdot h^{-1}$	This work
Cu-ZIF-400	0.20 g/L catalyst; 5.0 mM $Na_2S_2O_8$; 1.0 mM $[Ru(bpy)_3]Cl_2$; NaPi buffer solution (pH 7.0); LED ($\lambda \geq 420$ nm).	53.4 $\mu mol \cdot g^{-1} \cdot h^{-1}$	-	-	[1]
Au/CuO/Co_3O_4	10 mg catalyst; 1.0 M NaOH; 10 mL aqueous solution containing 0.1 M $Na_2S_2O_8$; 100 mW	2920 $\mu mol \cdot g^{-1} \cdot h^{-1}$	-	-	[2]

	Xe lamp.				
$CuCo_2O_4$	10 mg catalyst; 1 mmol $Na_2S_2O_8$; 10 mmol NaOH; 10 mL water; visible light irradiation ($\lambda > 420$ nm)	5100 $\mu mol \cdot g^{-1} \cdot h^{-1}$	-	-	[3]
g-C_3N_4/$Ni_xMo_{1-x}S_2$	-	-	10 mg catalyst; 20 mg EY; 30 mL 15% TEOA aqueous solution; 1 mL H_2PtCl_6 aqueous (1 mg/mL); 5 W LED lamp (420 nm).	9353.5 $\mu mol \cdot g^{-1} \cdot h^{-1}$	[4]
Cu@C/$SrTiO_3$	-	-	0.1 g catalyst; 0.85 g $AgNO_3$ (99.8%); 270 mL aqueous solution; 300 W Xe lamp ($\lambda \geq 400$ nm).	255.3 $\mu mol \cdot g^{-1} \cdot h^{-1}$	[5]
Cu-RSH	-	-	5 mg catalysts; 10 mg EY; 10 % TEOA in a mixed solvent of EtOH/H_2O (3:1); visible light ($\lambda \geq 420$ nm).	7880 $\mu mol \cdot g^{-1} \cdot h^{-1}$	[6]
Fe_3O_4/VAN@MIL-101(Fe)	1 mg catalyst; 1.0×10^{-3} M $[Ru(bpy)_3](ClO_4)_2$; 20 mM $Na_2S_2O_8$; 10 mL 80×10^{-3} M sodium borate buffer; Xe lamp ($\lambda \geq 420$ nm).	600 $\mu mol \cdot g^{-1} \cdot h^{-1}$	5 mg catalysts; 10% TEOA aqueous solution; Xe lamp ($\lambda \geq 420$ nm).	584 $\mu mol \cdot g^{-1} \cdot h^{-1}$	[7]
Co@CoO/NG	1.5 mg catalyst; 1.0mM $Ru(bpy)_3](ClO_4)_2$; 20 mM $Na_2S_2O_8$; 80 mM sodium borate buffer (pH 8.0); total reaction volume 10 ml; 300 W Xe lamp ($\lambda \geq 420$ nm).	543198 $\mu mol \cdot g^{-1} \cdot h^{-1}$	5 mg catalysts; 5 vol.% CH_3OH; total reaction volume 10 ml; 300 W Xe lamp ($\lambda \geq 420$ nm)	330 $\mu mol \cdot g^{-1} \cdot h^{-1}$	[8]

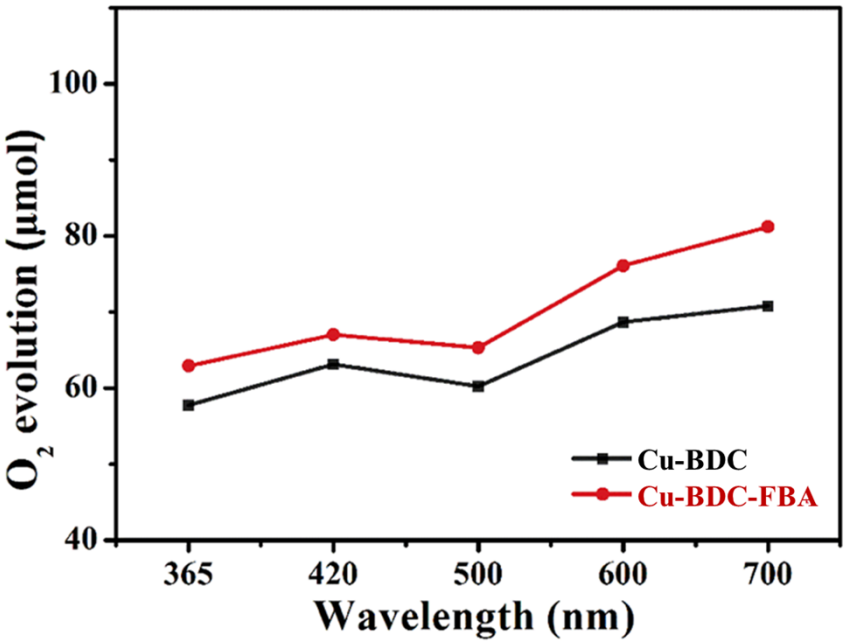

Fig. S6. Wavelength-dependent photocatalytic water oxidation results.

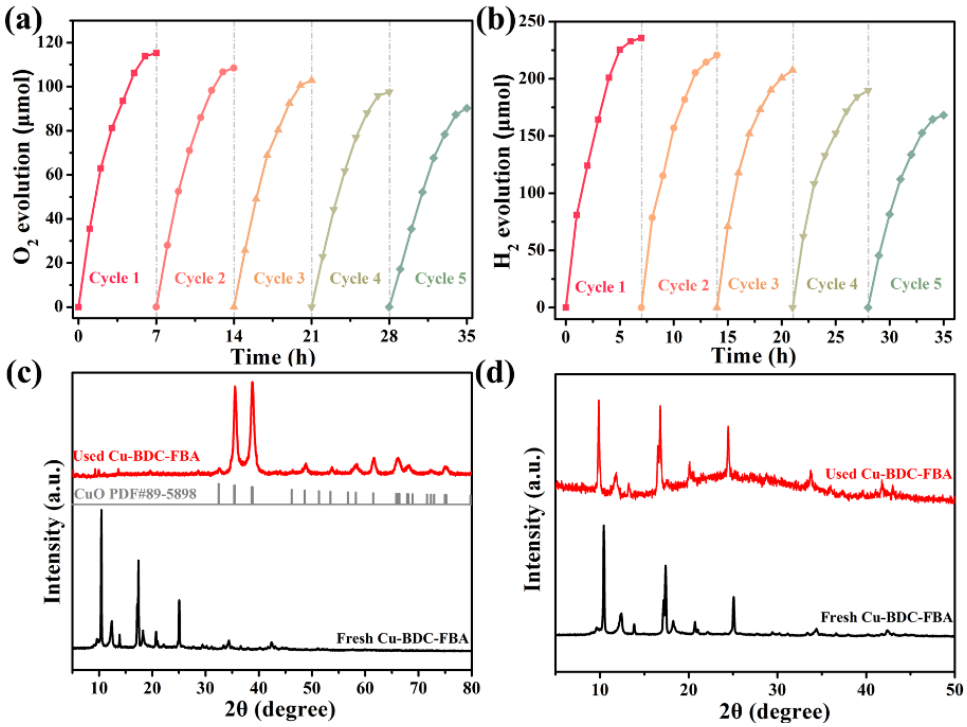

Fig. S7. (a) Recycle study of Cu-BDC-FBA in the light-driven water oxidation reaction; (b) Recycle study of Cu-BDC-FBA in the light-driven water reduction reaction; (c) Comparison of XRD patterns of fresh and reused Cu-BDC-FBA in water oxidation system; (d) Comparison of PXRD patterns of fresh and reused Cu-BDC-FBA in water reduction system.

References

1. Y. Zhang, X. Zhou, F. Zhang, T. Tian, Y. Ding and H. Gao, *J. Catal.*, 2017, **352**, 246-255.
2. G. Hu, C. Hu, Z. Zhu, L. Zhang, Q. Wang and H. Zhang, ACS Sustain. *Chem. Eng,*. 2018, **6**, 8801-8808.
3. E. Ding, A. Li, H. Liu, W. Liu, F. Chen, T. Li and B. Wang, *Nanoscale*, 2018, **10**, 3871-3876.
4. H. Yang, Z. Jin, H. Hu, Y. Bi and G. Lu, *Appl. Surf. Sci.*, 2018, **427**, 587-597.
5. L. Ren, L. Tong, X. Yi, W. Zhou, D. Wang, L. Liu and J. Ye, *Chem. Eng. J.*, 2020, **390**, 124558.
6. X.Y. Dong, M. Zhang, R.B. Pei, Q. Wang, D.H. Wei, S.Q. Zang, Y.T. Fan and T.C.W. Mak, *Angew. Chem. Int. Edit.*, 2016, **128**, 2113-2117.
7. Y. Guo, C. Feng, S. Qiao, S. Wang, T. Chen, L. Zhang, Y. Zhao and J. Wang, *Nanoscale*, 2020, **12**, 12551-12560.
8. S. Qiao, J. Guo, D. Wang, L. Zhang, A. Hassan, T. Chen, C. Feng, Y. Zhang and J. Wang, *In. J. Hydrogen Energy*, 2020, **45**, 1629-1639.